Thermodynamics, Kinetics, and Mechanism in Yeast Inorganic Pyrophosphatase Catalysis of Inorganic Pyrophosphate: Inorganic Phosphate Equilibration†

B. Springs, K. M. Welsh, and B. S. Cooperman*

ABSTRACT: We have developed two methods for quantitatively measuring inorganic pyrophosphate (PP_i) in the presence of 10^3–10^4 molar excesses of inorganic phosphate (P_i) and used them to measure the extent of enzyme-bound pyrophosphate (EPP_i) formation in solutions of yeast inorganic pyrophosphatase and P_i. We have also measured the rate of enzyme-catalyzed H_2O–phosphate oxygen exchange. We find both processes to have essentially identical dependence on Mg^{2+} and P_i concentrations, thus providing important confirmation for the recent proposal by Janson et al. (1979) that oxygen exchange proceeds via EPP_i formation. Our results are consistent with a model in which three Mg^{2+} per active site are required for EPP_i formation but inconsistent with a model requiring only two Mg^{2+} per active site and permit the formulation of an overall scheme for inorganic pyrophosphatase catalysis of PP_i–P_i equilibration as well as the evaluation of equilibrium and rate constants in this scheme. The major results and conclusions of our work are the following: (a) the equilibrium constant for PP_i (enzyme-bound) $\rightleftharpoons$ $2P_i$ (enzyme-bound) is 4.8; (b) following PP_i hydrolysis, the first released P_i contains an oxygen from solvent water; (c) the steps for PP_i hydrolysis on the enzyme and for release of both product P_i's are all partially rate determining in overall enzyme-catalyzed PP_i hydrolysis; (d) PP_i formation on the enzyme is rate determining for H_2O–P_i oxygen exchange; (e) PP_i dissociation from the enzyme is very slow and is the rate-determining step in P_i–PP_i exchange (Cohn, 1958; Janson et al., 1979). This also accounts for the observation that the calculated dissociation constant for $MgPP_i$ complex binding to enzyme is considerably lower than the measured K_m for enzyme-catalyzed $MgPP_i$ hydrolysis.

Yeast inorganic pyrophosphatase (EC 3.6.1.1) (PPase)[1] has long been known to catalyze both oxygen exchange between inorganic phosphate (P_i) and H_2O and inorganic pyrophosphate (PP_i)–P_i equilibration in addition to its catalysis of PP_i hydrolysis (Cohn, 1958). In this paper, we present a unified scheme for PPase action which accounts quantitatively for the observed overall rate constants of all three enzyme-catalyzed processes. PPase is a dimeric enzyme, made up of identical subunits (Heinrikson et al., 1973), which requires divalent metal ions for activity, with Mg^{2+} conferring the highest activity (Butler & Sperow, 1977; Janson et al., 1979). There is good evidence for the presence of two divalent metal ion sites (Rapoport et al., 1973), two P_i sites (Hamm & Cooperman, 1978), and one PP_i site (Ridlington & Butler, 1972) per subunit, but it has not been clear whether two, three, or even four divalent metal ions per subunit are required for enzymatic activity (Moe & Butler, 1972; Rapoport et al., 1972). Our data clearly favor a requirement for three metal ions.

In the work reported here, we have measured three different quantities: (a) enzyme-bound PP_i, which has led us to develop two convenient methods for quantitatively measuring PP_i in the presence of 10^3–10^4-fold molar excesses of P_i, (b) rates of H_2O–P_i oxygen exchange, using the ^{31}P NMR method of Cohn & Hu (1978), and (c) rates of $^{32}PP_i$ hydrolysis. We find enzyme-bound PP_i formation and the rate of enzyme-catalyzed H_2O–P_i oxygen exchange to have essentially identical dependence on the concentrations of both Mg^{2+} and P_i, in strong support of the idea recently proposed by Boyer and his coworkers (Hackney & Boyer, 1978; Janson et al., 1979) that oxygen exchange proceeds via enzyme-bound PP_i formation. As indicated above, our data are consistent with a model requiring three divalent metal ions per subunit for activity (and inconsistent with a model requiring only two) and, for this model, permit evaluation of all of the relevant equilibrium constants and all of the rate constants for enzyme-catalyzed $PP_i \rightleftharpoons 2P_i$ equilibration. In particular, we find the value for the equilibrium constant for PP_i (enzyme-bound) $\rightleftharpoons$ $2P_i$ (enzyme-bound) to be 4.8.

Experimental Procedures

Materials. Primary standard monobasic potassium phosphate was from Fisher Scientific. Carrier-free $^{32}P_i$ was from ICN (Riverside, CA). Carrier-free $^{32}PP_i$ was from New England Nuclear. ^{18}O-Enriched water (≥99%) was from either Prochem or Norsk-Hydro. D_2O (99.8%) was from Aldrich. Dowex 1 (1-X2, 100 mesh) and Dowex 50 (50-X8, 200 mesh) were from Bio-Rad. Bovine serum albumin (BSA) was from Sigma and was dialyzed against 100 mM Tris-HCl (pH 7.0) before use. All other chemicals were reagent grade and were used without further purification.

HN polygram Gel 300 PEI TLC sheets were from Brinkmann Instruments Inc. (Westbury, NY). Measurements of radioactivity were made by using an Intertechnique SL30 scintillation spectrometer. The scintillation cocktail contained 7 mL of a 3:1 toluene (0.5% PPO, 0.01% Me_2POPOP)–Triton X-100 mixture and 0.6 mL of H_2O.

Yeast inorganic pyrophosphatase was prepared as described previously and had a specific activity of 558–750 IU/mg as

† From the Department of Chemistry, University of Pennsylvania, Philadelphia, Pennsylvania 19104. *Received December 1, 1980; revised manuscript received June 17, 1981.* This work was supported by a research grant from the National Institutes of Health (AM-13212). ^{31}P NMR spectra were taken at the Middle Atlantic NMR Facility of the National Institutes of Health, located at the University of Pennsylvania.

[1] Abbreviations used: BSA, bovine serum albumin; PEI, poly(ethylenimine); P_i, inorganic phosphate; PP_i, inorganic pyrophosphate; PPase, yeast inorganic pyrophosphatase; Cl_3CCOOH, trichloroacetic acid; PPO, 2,5-diphenyloxazole; Me_2POPOP, 1,4-bis(4-methyl-5-phenyloxazol-2-yl)benzene; Tris, tris(hydroxymethyl)aminomethane; EDTA, ethylenediaminetetraacetic acid; Mes, 2-(*N*-morpholino)ethanesulfonic acid; $NaDodSO_4$, sodium dodecyl sulfate.

0006-2960/81/0420-6384$01.25/0

Table I: Stepwise Extraction of $^{32}P_i$ and $^{32}PP_i$ into 2-Methyl-1-propanol following Addition of Ammonium Molybdate

solution	total counts per minute	
	$^{32}P_i$	$^{32}PP_i$
initial aqueous	5.79×10^5	7.97×10^5
1[a]	5.67×10^5	7100
2	4849	2675
3	569	2155
4	145	2080
5	161	2375
final aqueous	339	7.82×10^5

[a] Solutions 1–5 correspond to each of the five 2-methyl-1-propanol layers.

measured by the standard titrimetric assay (Cooperman et al., 1973).

Methods. Determination of Enzyme-Bound PP_i. PPase, typically at a concentration of 100 μM, was incubated with $^{32}P_i$ and Mg^{2+} in buffer for 1 h (actually equilibration is reached in $\leq$1 min) at 25 °C in a total volume of 40 μL, and the solution was quenched by addition of 15 μL of 4 M trichloroacetic acid (Cl_3CCOOH). Separately an equivalent amount by weight of BSA and a trace of enzyme (0.01–0.001 μM) to equilibrate P_i and PP_i were incubated with $^{32}P_i$ and Mg^{2+} under identical conditions. This solution serves as a background control. Cold carrier P_i and PP_i were added to each sample, and the amount of $^{32}PP_i$ in each was determined by two different methods. The first involves the selective extraction into 2-methyl-1-propanol from water of $^{32}P_i$ as a phosphomolybdate complex leaving behind $^{32}PP_i$ in the aqueous solution. The second method involves the separation of PP_i from P_i by two-dimensional TLC on PEI plates.

Selective Extraction Method. Following Cl_3CCOOH addition, samples, typically containing 10^6–10^7 cpm, are centrifuged, and the supernatants are transferred to tared culture tubes containing 5 mL of 0.1 mM P_i and 0.1 mM PP_i. The total amount of aqueous solution is determined by weight, and an aliquot is counted for radioactivity, giving the total counts per minute present before extraction, denoted C_1. To each tube is added 1 mL of 2% ammonium molybdate in 2 N H_2SO_4, and the resulting aqueous solution is then extracted 6 times with 5-mL portions of 2-methyl-1-propanol. After all but the sixth extraction, 100 μL of 5 mM P_i is added as a nonradioactive carrier. After the second and fourth extractions, 1 mL of H_2O is added to maintain the volume of the aqueous solution. Following the sixth extraction, the tubes are reweighed to determine the net aqueous weight, and an aliquot is counted for radioactivity, allowing calculation of the total counts per minute present after extraction, denoted C_2. The ratio $C_2/2C_1$ is equal to the $[^{32}PP_i]/[^{32}P_i]$ present in the initial Cl_3CCOOH supernatant, and since $[^{32}P_i]$ is known, $[^{32}PP_i]$ is determined. Estimates of enzyme-bound PP_i are determined by subtracting the $[^{32}PP_i]$ in the background control from $[^{32}PP_i]$ in the PPase-containing sample. Reproducibility was ±9%.

The selectivity of the extraction is illustrated by data presented in Table I, which shows the radioactivity in each of five successive 2-methyl-1-propanol layers following extraction of solutions of $^{32}P_i$ and, separately, $^{32}PP_i$ as well as in the aqueous layers before and following the five extractions.

TLC Method. Following incubation, Cl_3CCOOH quenching, and centrifugation as described above, a 30-μL aliquot of the supernatant, typically containing 5×10^7 cpm, was diluted with an equal volume of a solution containing 53 mM EDTA, 7 mM PP_i, 1.6 M KOH, and 27 mM Tris (pH 7.0), and an aliquot was applied to a 10 × 10 cm TLC sheet which had been previously washed in 10% NaCl and H_2O to remove impurities (Randerath & Randerath, 1967).

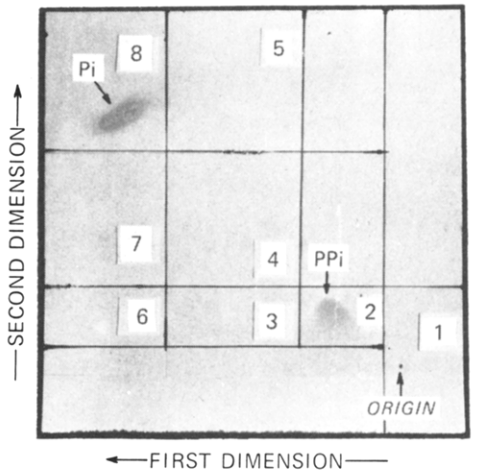

FIGURE 1: Typical plate following two-dimensional TLC. Dark spots show areas of staining following spraying with molybdate reagent and correspond to P_i and PP_i as indicated. The numbered boxes are separately cut out and counted for radioactivity.

Table II: Distribution of Radioactivity (cpm) following Two-Dimensional TLC

box no.[a]	applied solutions[b]		
	A (P_i alone)	B (PP_i alone)	C (P_i and PP_i)
1	904	81	990
2	652	6452	7332
3	282	45	2216
4	3755	44	4201
5	252	52	1973
6	7771	80	3.7×10^5
7	1.695×10^6	107	
8	0.865×10^6	218	2.08×10^6[c]

[a] See Figure 1. [b] Solutions A and C contained 2.50×10^6 cpm of $^{32}P_i$. Solutions B and C contained 7000 cpm of $^{32}PP_i$. [c] Boxes 7 and 8 counted together.

The TLC sheet was eluted in the first dimension in 1 M LiCl, air-dried, rotated 90°, eluted with 1:1 MeOH–H_2O to remove LiCl, air-dried, and eluted in the second dimension with 1 M LiCl. P_i- and PP_i-containing spots were located by spraying with a molybdate reagent (72% perchloric acid–1 N HCl–4% ammonium molybdate–H_2O, 5:10:25:60; Bandurski & Axelrod, 1951) and heating in a drying oven at 80–100 °C for a few minutes. The TLC sheet was cut into sections (Figure 1), and each section was placed in a scintillation vial, covered with scintillation cocktail, and counted for radioactivity. That this method is able to separate PP_i from excess P_i is shown by analysis of three test solutions containing $^{32}P_i$, $^{32}PP_i$, and a mixture of $^{32}P_i$ and $^{32}PP_i$, respectively (Table II). For the $^{32}P_i$ solution, 99.5% of the radioactivity is found in boxes 7 and 8. For the $^{32}PP_i$ solution, 91% of the radioactivity is found in box 2, and 5% of the radioactivity, representing contaminating $^{32}P_i$, migrates to boxes 7 and 8. The amount of $^{32}PP_i$ in the mixed solution due to added $^{32}PP_i$ is given by the radioactivity in box 2 for column C minus the radioactivity in box 2 for column A (6680 cpm) and is equal within experimental error to the radioactivity in box 2 for column B (6452 cpm). We found that the energy of ^{32}P decay on a TLC plate is lower than it is in solution, with the result that much of the radioactivity did not get counted when the normal ^{32}P window settings of the SL-30 spectrometer were used. Accordingly, the window was set wide open to determine the ^{32}P radioactivity on a TLC plate. Radioactivity in boxes including

Table III: Measurement of Inorganic Pyrophosphatase Bound PP_i by Both Methods[a]

method	found $[PP_i]/[P_i]$	background $[PP_i]/[P_i]$	corrected bound $[PP_i]/[P_i]$	$[PP_i]/[PPase]_{total}$
extraction	$(0.452 \pm 0.006) \times 10^{-3}$	$(0.049 \pm 0.003) \times 10^{-3}$	$(0.403 \pm 0.007) \times 10^{-3}$	0.118
TLC	$(0.560 \pm 0.061) \times 10^{-3}$	$(0.096 \pm 0.027) \times 10^{-3}$	$(0.464 \pm 0.067) \times 10^{-3}$	0.136

[a] The reaction mixture included 30 mM P_i, 15 mM Mg^{2+}, 200 mM KCl, 50 mM Tris (pH 7.0), and 102 μM inorganic pyrophosphatase calculated as in Figure 2.

and adjacent to the P_i spot was used to determine total $^{32}P_i$. Radioactivity in the box containing the PP_i spot was used to determine $^{32}PP_i$. A corrected $[PP_i]/[P_i]$ ratio was obtained by subtracting the value for a background control sample from the value for a reaction mixture, as described above. All solutions were spotted in triplicate or quadruplicate. Corrected $[PP_i]/[P_i]$ ratios were reproducible within ±12%.

Rates of H_2O–P_i Oxygen Exchange. Rates of H_2O–P_i oxygen exchange were determined by measuring ^{18}O release from ^{18}O-labeled P_i with the NMR method of Cohn & Hu (1978), which resolves the ^{31}P peaks due to the five ^{18}O-labeled and unlabeled species, designated $P^{18}O_0$, $P^{18}O_1$, $P^{18}O_2$, $P^{18}O_3$, and $P^{18}O_4$ (Hackney & Boyer, 1978). ^{18}O-Labeled P_i (93 ± 6% $P^{18}O_4$ and 7 ± 6% $P^{18}O_3$) was prepared according to Hackney et al. (1980) with the modification that the Dowex 1 resin was base-washed prior to pouring the column. The collected P_i fractions were titrated to pH 4.0 with KOH, lyophilized, redissolved in H_2O, titrated to pH 7.0, and centrifuged to remove insoluble material. The P_i content of the supernatant was determined colorimetrically by using the procedure of Josse (1966), with the modification that the incubation was carried out at 40 °C. Reaction solutions containing ^{18}O-labeled P_i (6.4–100 mM) and PPase were incubated at 25 °C. At various times, aliquots containing 22 μmol of P_i were removed, and the reaction was quenched by rapid mixing with HCl and $NaDodSO_4$ to final concentrations of 2 N HCl and 0.15% $NaDodSO_4$. After standing for at least 3 h at room temperature, the quenched aliquot was passed through a Dowex 50 column (6 × 70 mm) and eluted with 1 N HCl. The collected P_i-containing fractions were adjusted to pH 9 with NaOH or KOH, and the lyophilized material was redissolved in 1.5 mL of 30–50% D_2O, such that the final P_i concentration was 15 mM, and centrifuged to remove insoluble material. EDTA (15 μmol) was then added, and the sample was transferred to a 10-mm NMR tube equipped with a vortex plug.

NMR spectra were taken on a Bruker WH-360 at 145.732 MHz. The acquisition time was 3.4 s with a pulse angle of 90°. Integration of peaks was by planimetry. Apparent rate constants for overall ^{18}O exchange were calculated as the slopes of plots of ln (average ^{18}O content of P_i) vs. time, where

$$\text{average } ^{18}\text{O content of } P_i = \frac{4[P^{18}O_4] + 3[P^{18}O_3] + 2[P^{18}O_2] + [P^{18}O_1]}{4([P^{18}O_4] + [P^{18}O_3] + [P^{18}O_2] + [P^{18}O_1] + [P^{18}O_0])} \quad (1)$$

Rate constants for $P^{18}O_4$ disappearance were calculated as the slopes of plots of $-\ln([P^{18}O_4]_0/[P^{18}O_4]_t)$ vs. time.

Rates of PP_i Hydrolysis. Initial rate measurements of enzyme-catalyzed PP_i hydrolysis were made by using $^{32}PP_i$ at a specific radioactivity of 10^4–10^6 cpm/nmol. Solutions containing $MgCl_2$ (10, 30, or 100 mM), KCl (200 mM), and varying concentrations of $NaPP_i$ (1.7–1000 μM) in Tris-HCl buffer (0.05 M, pH 7.0) were preincubated at 25 °C. Reactions were initiated on addition of PPase and quenched by addition of an equal volume of 1.5 M Cl_3CCOOH. To 0.1-mL aliquots of quenched reaction were added 5 mL of a solution containing 0.1 mM KP_i and 0.1 mM $NaPP_i$ and then 1 mL of 2% ammonium molybdate in 2 N H_2SO_4. The mixture was extracted with 5 mL of 2-methyl-1-propanol, and the radioactivity in the 2-methyl-1-propanol layer, which provides a measure of $^{32}P_i$–molybdate and thus of enzyme-catalyzed $^{32}PP_i$ hydrolysis, was determined.

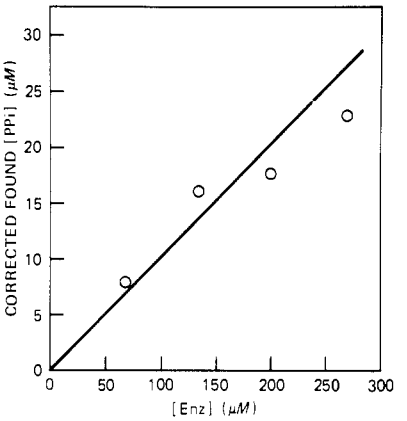

FIGURE 2: Dependence of PP_i formation on PPase concentration. All solutions contained 10 mM Mg^{2+}, 20 mM P_i, and 82 mM Tris (pH 7.0). Enzyme concentration is based on a subunit molecular weight of 35000 (Heinrikson et al., 1973) and an $A_{280}^{1\%}$ of 14.5 (Kunitz, 1952).

Results

Equilibrium Formation of Enzyme-Bound Inorganic Pyrophosphate. In agreement with the results of Janson et al. (1979), we find that PPase stimulates formation of PP_i from P_i. Most of the measurements we report in this paper were obtained by using the selective extraction method, because it can be performed more rapidly than the TLC method. Proof that the extraction method is indeed measuring PP_i is provided by the agreement, within experimental error, of the results obtained when a common solution is analyzed by both the TLC and extraction methods, as seen in Table III.

The amount of enzyme-dependent PP_i formed is proportional to PPase (Figure 2) and reflects PP_i bound to PPase, as previously demonstrated (Janson et al., 1979). Henceforth we denote total concentration of PP_i bound to PPase as $[EPP_i]_t$, where the subscript t refers to all forms without regard to protonation state or stoichiometry of bound Mg^{2+}. The total enzyme concentration in a reaction mixture is denoted $[E]_T$.

The dependence of the ratio $[EPP_i]_t/[E]_T$ was investigated as a function of Mg^{2+}, P_i, and KCl concentrations. If total Mg^{2+} concentration, $[Mg]_T$, is maintained fixed at 10 mM, PP_i formation goes through a maximum as a function of total P_i concentration, $[P_i]_T$, and increases as a function of $[P_i]_T$ more rapidly in the absence than in the presence of KCl (Figure 3). If free Mg^{2+} concentration, $[Mg]_{free}$, is maintained constant, in the range 5–30 mM, then apparently simple saturation curves are obtained as a function of total P_i concentration (Figure 4a). Although half-maximal EPP_i formation is obtained at lower $[P_i]_T$ as $[Mg]_{free}$ is raised, maximal EPP_i formation is essentially independent of $[Mg]_{free}$, between 10 and 30 mM, but it is dependent on $[Mg]_{free}$ at lower levels,

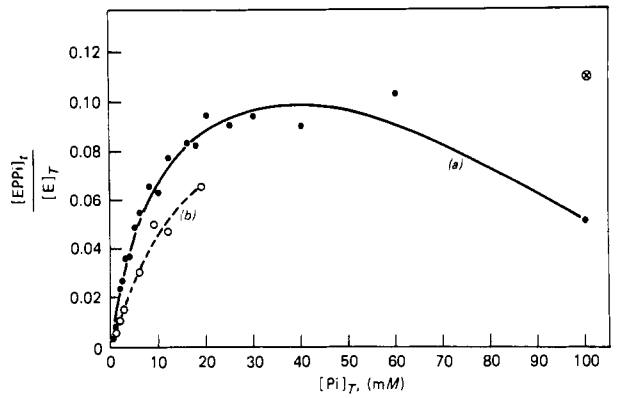

FIGURE 3: Dependence of $[EPP_i]_t/[E]_T$ on $[P_i]_T$ at fixed $[Mg]_T$. All solutions contained 10 mM Mg^{2+}, except as indicated, 50 mM Tris (pH 7.0), and 140 μM PPase. (Curve a) No added KCl. (Curve b) Plus 0.2 M KCl. The point marked by × was measured in a solution containing 20 mM Mg^{2+} in the absence of KCl.

as shown by the results obtained at 5 mM. This is also shown by the decrease in EPP_i formation with increasing P_i concentration at fixed $[Mg]_T$ and by the increase in EPP_i formation at high P_i concentration on addition of Mg^{2+} (Figure 3). Finally, if the data in Figure 4A are replotted as a function of MgP_i complex concentration [calculated by taking K_B (Table V) equal to 50 mM (Table VIII)] (Figure 4B), the curves at 10 and 30 mM $[Mg]_{free}$ are seen to be essentially superimposable. From these studies, we conclude that the formation of EPP_i depends on $[MgP_i]$. The apparent tighter binding of P_i in the absence of KCl (Figure 1) is at least partly attributable to the effect of added KCl in increasing the dissociation constant for the MgP_i complex.

A simple scheme for EPP_i formation is shown in eq 2. The

$$E + P_i \rightleftharpoons EP_i + P_i \rightleftharpoons E(P_i)_2 \rightleftharpoons EPP_i \quad (2)$$

$$[E]_T = [E]_t + [EP_i]_t + [E(P_i)_2]_t + [EPP_i]_t \quad (3)$$

conservation equation for enzyme is then given by eq 3, where the subscript t refers, as above, to all forms of a particular species without regard to stoichiometry of bound Mg^{2+} or protonation state, and the equation for EPP_i formation at equilibrium in reciprocal form is given by eq 4, where A and

$$\frac{[E]_T}{[EPP_i]_t} = \frac{A}{[P_i]_T^2} + \frac{B}{[P_i]_T} + C \quad (4)$$

B are complex parameters and C is the limiting value of $[E]_T/[EPP_i]_t$ at saturating $[P_i]_T$. Because of our results (Figure 4B) showing EPP_i formation to depend on $[MgP_i]$, we choose to rewrite eq 4 as

$$\frac{[E]_T}{[EPP_i]_t} = \frac{A}{[MgP_i]^2} + \frac{B}{[MgP_i]} + C \quad (5)$$

Table IV: Values for Parameters A, B, and C (eq 5), for K_m and k_{cat} for H_2O–P_i Oxygen Exchange, and for K_m and k_{cat} for PP_i Hydrolysis

	KCl (mM)	$[Mg^{2+}]_{free}$ (mM) 10	30	100
A (mM^2)	200	2.11	7.2	
B (mM)	200	21.1	22.5	
C	200	5.9	5.7	
K_m (exchange) (mM)	200	3.3	3.8	
k_{cat} (exchange) (s^{-1})	200	171	174	
K_m (hydrolysis) (μM)	200	7.1 ± 1.0	4.5 ± 0.5	6 ± 2
k_{cat} (hydrolysis) (s^{-1})	200	212 ± 20	138 ± 35	131 ± 35
K_m (hydrolysis) (μM)	0	4.7		
k_{cat} (hydrolysis) (s^{-1})	0	150		

Plots of $[E]_T/[EPP_i]_t$ vs. $1/[MgP_i]$ show curvature, as predicted from eq 5, but are linear at relatively high $[MgP_i]$ where the term $A/[MgP_i]^2$ becomes negligible (Figure 5A), allowing rather good estimates of C to be made. With C determined, eq 5 can be rewritten as eq 6, allowing values of

$$[MgP_i]\left(\frac{[E]_T}{[EPP_i]_t} - C\right) = \frac{A}{[MgP_i]} + B \quad (6)$$

A and B to be estimated graphically (Figure 5B). Values of A, B, and C for $[Mg]_{free}$ equal to 10 or 30 mM, as determined from Figure 5A,B, are listed in Table IV. The significance of these values is discussed below.

Rate of Water–P_i Oxygen Exchange. The rate of enzyme-catalyzed oxygen exchange between water and P_i (V_{ex}) was determined as a function of $[MgP_i]$ at $[Mg]_{free}$ concentrations of 10 and 30 mM in reaction mixtures paralleling exactly those used for measurement of enzyme-bound PP_i. Data were taken at $[MgP_i] \geq 1$ mM. In this range, plots of $1/V_{ex}$ vs. $1/[MgP_i]$ were found to be linear, yielding the K_m and k_{cat} values shown in Table IV. The closely similar dependence of both the rate of H_2O–P_i oxygen exchange and the extent of EPP_i formation on $[MgP_i]$ is shown explicitly in Figure 6, in which $V_{max,ex}/V_{ex}$ and $[E]_T/C[EPP_i]_t$ are each plotted vs. $1/[MgP_i]$. The observed differences in slope (23% at 10 mM $[Mg]_{free}$ and 21% at 30 mM $[Mg]_{free}$) fall within the combined experimental errors of the two determinations.

Hackney & Boyer (1978) have defined a partition coefficient, P_c, for enzyme-catalyzed H_2O–P_i oxygen exchange, as the rate at which enzyme-bound P_i loses water in the exchange step divided by the sum of this rate and the rate of release of P_i to the medium and have shown how P_c can be calculated from the ratio of the rate of $P^{18}O_4$ disappearance to the rate of overall oxygen exchange. From our measurements, we

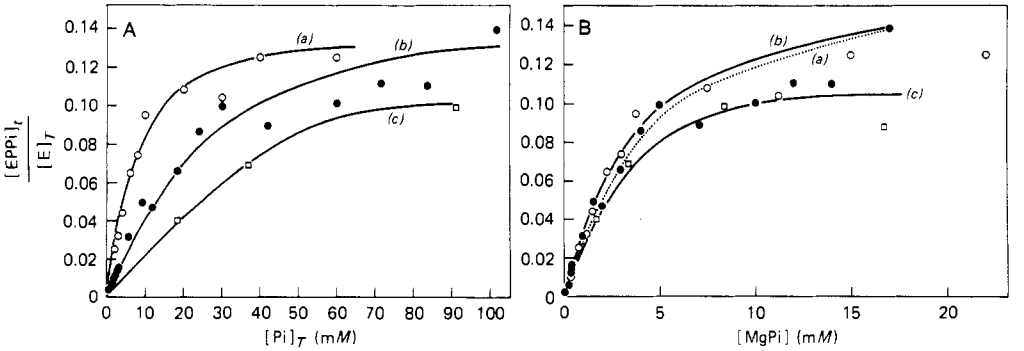

FIGURE 4: Dependence of $[EPP_i]_t/[E]_T$ on $[P_i]_T$ or $[MgP_i]$ at different $[Mg]_{free}$. All solutions contained 50 mM Tris (pH 7.0), 0.2 M KCl, 140 μM PPase, and sufficient Mg^{2+} to maintain a fixed level of $[Mg]_{free}$. The $[Mg]_{free}$ levels were (a) 30, (b) 10, and (c) 5 mM. In part B, curves a and b are drawn according to eq 5 by using the values for A, B, and C listed in Table IV.

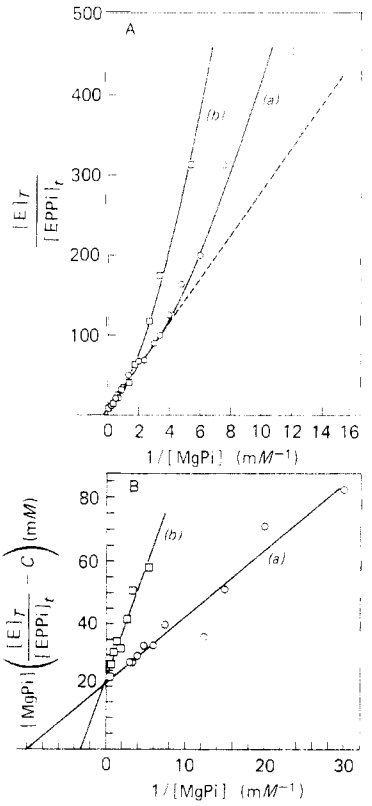

FIGURE 5: Dependence of $[E]_T/[EPP_i]_t$ and $[MgP_i]([E]_T/[EPP_i]_t - C)$ on $1/[MgP_i]_t$ at different $[Mg]_{free}$. The lines are drawn according to eq 5 and 6 by using the values for A, B, and C listed in Table IV. The $[Mg]_{free}$ levels are (a) 10 and (b) 30 mM.

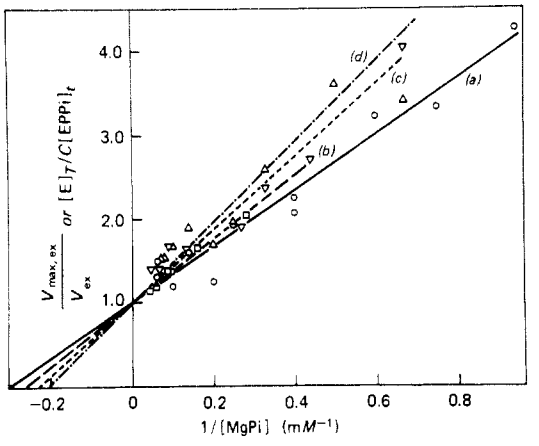

FIGURE 6: Plots of $[E]_T/C[EPP_i]_t$ and $V_{ex,max}/V_{ex}$. (a) $V_{ex,max}/V_{ex}$, $[Mg]_{free}$, 10 mM (○); (b) $V_{ex,max}/V_{ex}$, $[Mg]_{free}$, 30 mM (□--□); (c) $[E]_T/C[EPP_i]_t$, $[Mg]_{free}$, 10 mM (△---△); (d) $[E]_T/C[EPP_i]_t$, $[Mg]_{free}$, 30 mM (▽-·-▽). Experimental conditions are as in Figure 3, except that $[E]_T$ ranged from 0.3 to 0.6 μM for curves a and b.

obtain a P_c value of 0.23 ± 0.07 over a range of $[MgP_i]$ from 0.7 to 16.7 mM, with no trend in the value of P_c over this concentration range. These results agree within experimental error with those recently obtained by Hackney (1980), by mass spectral analysis of P_i produced by PPase catalysis of P_i–H_2O oxygen exchange, who reported a P_c value, measured at pH 7.1, of 0.30 ± 0.01 over a range of P_i concentration.

Initial Rates of PP_i Hydrolysis. Initial rates of $^{32}PP_i$ hydrolysis were measured as a function of PP_i concentration at 10, 30, and 100 mM $[Mg]_T$ in the presence of added KCl and at 10 mM $[Mg]_T$ in the absence of added KCl. The data obtained, when plotted according to Eadie–Hofstee, yielded the values for apparent K_m (based on $[PP_i]_T$) and k_{cat} shown in Table IV. The small decrease in V_{max} on going to higher

Scheme I: Possible Enzyme Species Present in Solutions Containing PPase, Mg^{2+}, P_i, and PP_i[a]

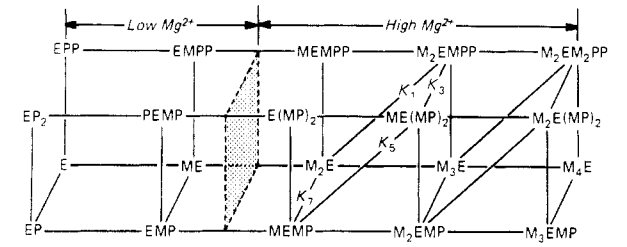

[a] Equilibrium constants are defined in Table II.

$[Mg]_T$ as well as the lack of clear trend in apparent K_m in the $[Mg]_T$ range studied is consistent with results reported earlier by Moe & Butler (1972), who worked at a slightly higher pH (pH 7.4).

Discussion and Interpretation of Results

In this section, we first show that the measured values for the parameters A, B, and C in eq 5, which are listed in Table IV, are consistent with a model in which three Mg^{2+} per active subunit are required for EPP_i formation from P_i, and a fourth Mg^{2+} may be bound at high Mg^{2+} concentrations but is not required for EPP_i formation or hydrolysis, but are inconsistent with a model in which only two Mg^{2+} per active subunit are required. We then present the minimal scheme consistent with our results for PPase catalysis of PP_i–$2P_i$ equilibration, evaluate the equilibrium and all of the rate constants in this scheme, and discuss some of its mechanistic aspects.

Solutions containing PPase, Mg^{2+}, PP_i, and P_i contain a total of 20 possible enzyme species, assuming 1 PP_i, 2 P_i, and up to 4 Mg^{2+} binding sites per subunit and that P_i and PP_i binding are mutually exclusive[2] (Scheme I). PPase devoid of P_i or PP_i is known to bind 2 mol of Mg^{2+} or other divalent metal ions per subunit, with the weaker affinity site having an apparent K_D for Mg^{2+} of 0.2 mM at pH 7 (Rapoport et al., 1973). Furthermore, results obtained in this laboratory show that enzyme affinity for divalent metal ion increases in the presence of P_i (Cooperman et al., 1981). Thus for $[Mg]_{free}$ equal to 10–30 mM, only the 12 enzyme species to the right in Scheme I are potentially stoichiometrically significant, so that the following conservation equations hold:

$$[Mg]_T = [Mg]_{free} + [MgP_i] \quad (7)$$

$$[P_i]_T = [P_i] + [MgP_i] \quad (8)$$

$$[E]_T = [Mg_2E] + [Mg_3E] + [Mg_4E] + [MgEMgP_i] + [Mg_2EMgP_i] + [Mg_3EMgP_i] + [E(MgP_i)_2] + [MgE(MgP_i)_2] + [Mg_2E(MgP_i)_2] + [MgEMgPP_i] + [Mg_2EMgPP_i] + [Mg_2EMg_2PP_i] \quad (9)$$

where the bracketed concentration terms refer only to stoichiometries and not to the relative physical arrangements of Mg^{2+}, P_i, and PP_i on the enzyme. Thus, for example, $MgEMgP_i$ refers to an enzyme subunit binding two Mg^{2+} and one P_i, and does not signify that there is necessarily an enzyme-bound Mg^{2+}–P_i complex.

The relevant equilibrium constants are defined in Table V, and expressions for parameters A, B, and C, when all 12 enzyme species listed in eq 9 are considered to be stoichiometrically significant, are given in Table VI. Empirically, we find (Table IV) that parameter A is approximately proportional to $[Mg]_{free}$ whereas parameters B and C are essen-

[2] We have recently shown that P_i is a competitive inhibitor of PP_i.

Table V: Definitions of Apparent Equilibrium Constants (pH 7.0)

$K_A = [Mg][PP_i]/[MgPP_i]$ $K_M = [Mg][E]/[MgE]$
$K_{A_2} = [Mg][MgPP_i]/[Mg_2PP_i]$ $K_{M_2} = [Mg][MgE]/[Mg_2E]$
$K_B = [Mg][P_i]/[MgP_i]$ $K_{M_3} = [Mg][Mg_2E]/[Mg_3E]$
$K_{PP} = [P_i]^2/[PP_i]$ $K_{M_4} = [Mg][Mg_3E]/[Mg_4E]$

$K_1 = [Mg_2E][MgPP_i]/[Mg_2EMgPP_i]$
$K_3 = [MgE(MgP_i)_2]/[Mg_2EMgPP_i]$
$K_5 = [MgEMgP_i][MgP_i]/[MgE(MgP_i)_2]$
$K_7 = [Mg_2E][P_i]/[MgEMgP_i]$

$K_M^{PP} = [Mg][MgEMgPP_i]/[Mg_2EMgPP_i]$
$K_M^{P_2} = [Mg][E(MgP_i)_2]/[MgE(MgP_i)_2]$
$K_M^{P} = [Mg][MgEMgP_i]/[Mg_2EMgP_i]$
$K_{M_2}^{PP} = [Mg][Mg_2EMgPP_i]/[Mg_2EMg_2PP_i]$
$K_{M_2}^{P_2} = [Mg][MgE(MgP_i)_2]/[Mg_2E(MgP_i)_2]$
$K_{M_2}^{P} = [Mg][Mg_2EMgP_i]/[Mg_3EMgP_i]$

tially independent of $[Mg]_{free}$. In order to be consistent with the expressions in Table VI, these results require that one of the three models shown in Table VII apply for $[Mg]_{free}$ in the range 10–30 mM. These models have in common those forms of the enzyme having two bound P_i's or one bound PP_i containing one additional Mg^{2+} as compared with forms containing one P_i or neither P_i nor PP_i, with the result that $E(MgP_i)_2$, $MgEMgPP_i$, Mg_4E, and Mg_3EMgP_i are stoichiometrically unimportant. Designating the four stoichiometrically important species of model 1 as set 1 and those of model 2 as set 2, we note that an important property of model 3 in that although the relative amount of set 1 as compared with set 2 will depend on the ratio of $[Mg]_{free}$ to the common dissociation constant, K_0, the relative amounts of $[E]_t$, $[EP_i]_t$, $[E(P_i)_2]_t$, and $[EPP_i]_t$ (see eq 3) are independent of $[Mg]_{free}$. Although our studies on EPP_i formation do not distinguish among these models, a choice in favor of model 3 can be made on the basis of the results of two other experiments. The binding studies of Rapoport et al. (1973), which our more recent studies support (Cooperman et al., 1981), show that two Mg are bound per enzyme subunit at $[Mg]_{free}$ of ~1 mM and show no evidence for formation of Mg_3E. Thus, 10 mM $[Mg]_{free}$ could not be $\gg K_{M_3}$, which rules out model 2. In addition, model 1 provides no explanation for the observed decrease in k_{cat} (hydrolysis) as $[Mg]_{free}$ is raised from 10 to 30–100 mM (Table IV; Moe & Butler, 1972). By contrast, both of these results are consistent with model 3 if it is assumed that $K_0 \gg 1$ mM [our data and those of Moe & Butler (1972) suggest a value of approximately 10–20 mM] and that Mg_2EMgPP_i hydrolyzes somewhat more rapidly than does $Mg_2EMg_2PP_i$. We conclude that model 3 is correct.

Previous studies (Kunitz, 1952; Moe & Butler, 1972), which are in accord with the results we have obtained,[3] have shown that optimal pyrophosphate hydrolysis activity occurs at $[Mg]_{free}$ of about 1 mM. At this Mg level, our approximate K_0 value would require that the dominant species in solution were those included in set 1. Recent equilibrium dialysis results in our laboratory, showing that for $[Mn^{2+}]$ or $[Co^{2+}] < 1$ mM, in the presence of P_i up to 3 mol of $^{54}Mn^{2+}$ or $^{57}Co^{2+}$ can be bound per PPase subunit whereas in the absence of P_i only 2 mol of $^{54}Mn^{2+}$ or $^{57}Co^{2+}$ are bound, support this conclusion (Cooperman et al., 1981).

At higher $[Mg]_{free}$ levels, (>30 mM), model 3 predicts that the dominant species would be those included in set 2, which differs from set 1 in that all the forms of enzyme differing in P_i or PP_i content contain an additional Mg^{2+}. However, the relative independence of the parameters listed in Table IV as a function of $[Mg^{2+}]$ (10–100 mM) strongly suggests that this additional Mg^{2+} has no catalytic function and binds at a site unrelated to the active site. Accordingly, it will be ignored in the discussion that follows.

[3] K. M. Welsh and B. S. Cooperman, unpublished observations.

Scheme II: Overall Thermodynamic Scheme for Enzyme-Catalyzed $PP_i \rightleftharpoons 2P_i$ Equilibration[a]

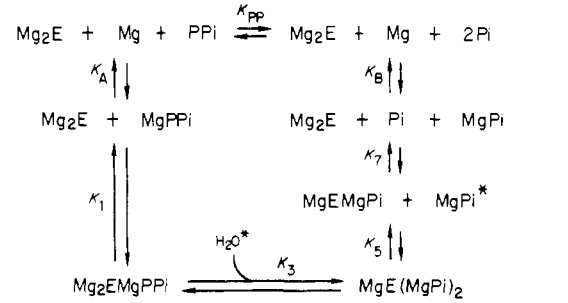

[a] The first P_i released following hydrolysis of PP_i is the one which exchanges oxygen with H_2O (see text).

We may now write a minimal overall thermodynamic scheme for PPase catalysis of PP_i–$2P_i$ equilibration as Scheme II, where the values for the relevant equilibrium constants are shown in Table VIII. From Table VI, for model 3, K_3 is equal to $C - 1$, K_5 is equal to $B/(C - 1)$, and K_7 is equal to $AK_B/B[Mg]_{free}$. The value $K_3 = 4.8$ shows that on the enzyme surface there is only a small negative free-energy change on PP_i hydrolysis (-0.9 kcal/mol). This is analogous to the small free-energy changes accompanying myosin-bound ATP hydrolysis (Bagshaw & Trentham, 1973) as well as phosphoryl transfer from ATP bound to several kinases (Cohn, 1979; Knowles, 1980), and accounts for the high activity of PPase in catalyzing H_2O–P_i oxygen exchange. The constants K_{PP}, K_A, and K_B were estimated at pH 7.0 and 0.2 M KCl from literature values. K_1, calculated from eq 10, is equal to 0.2 μM (Table VIII).

$$K_1 = \frac{K_3 K_5 K_7 K_B}{K_A K_{PP}} \quad (10)$$

According to Scheme II, H_2O–P_i oxygen exchange catalyzed by PPase proceeds via enzyme-bound PP_i formation. This was recently proposed by Boyer and his co-workers (Hackney & Boyer, 1978; Janson et al., 1979) on the basis of their demonstration of EPP_i formation from PPase and P_i, the similarity in P_c values for enzyme catalysis of both PP_i hydrolysis and P_i–H_2O oxygen exchange, and the demonstration that the formation of enzyme-bound PP_i from P_i was kinetically competent as an intermediate in P_i–H_2O exchange. Our results (Figure 6) showing essentially identical dependence of both the amount of enzyme-bound PP_i formation and the rate of P_i–H_2O oxygen exchange on the concentration of MgP_i is strong independent support for their proposal. It should also be noted that the pH dependence of V_{max} for PPase-catalyzed P_i–H_2O oxygen exchange is similar to that of V_{max} for PPase-catalyzed PP_i hydrolysis, showing an optimum near pH 7.0 and falling off more rapidly on the acid than on the alkaline side.[3]

It is of interest to determine which of the two P_i sites on PPase contains the electrophilic P_i which exchanges an oxygen on PP_i hydrolysis or formation, and which of the sites contains the leaving group (in PP_i hydrolysis) or nucleophilic (in PP_i formation) P_i, which retains all of its oxygen during enzyme catalysis.[4] From Scheme II, if the electrophilic P_i is released

[4] Hackney (1980) has shown that the two bound phosphates do not equilibrate on the enzyme surface.

Table VI: Definition of Parameters A, B, and C

parameter	full definition	definition for model 3
A	$\frac{K_{M_2}^{PP}K_3K_5K_7[Mg]^2(K_{M_3}K_{M_4} + K_{M_4}[Mg] + [Mg]^2}{K_{M_4}K_{M_3}K_B(K_M^{PP}K_{M_2}^{PP} + K_{M_2}^{PP}[Mg] + [Mg]^2}$	$\frac{K_3K_5K_7}{K_B}[Mg]$
B	$\frac{K_{M_2}^{PP}K_3K_5[Mg](K_M^{P}K_{M_2}^{P} + K_{M_2}^{P}[Mg] + [Mg]^2)}{K_{M_2}^{P}K_M^{P}(K_M^{PP}K_{M_2}^{PP} + K_{M_2}^{PP}[Mg] + [Mg]^2)}$	K_3K_5
C	$\frac{K_{M_2}^{PP}K_3(K_M^{P_2}K_{M_2}^{P_2} + K_{M_2}^{P_2}[Mg] + [Mg]^2)}{K_{M_2}^{P_2}(K_M^{PP}K_{M_2}^{PP} + K_{M_2}^{PP}[Mg] + [Mg]^2)} + 1$	$K_3 + 1$

Table VII: Possible Models for Ligand Binding to PPase

model	relationships	dominant stoichiometric species
1	$K_{M_3}, K_{M_4}, K_M^{P}, K_{M_2}^{P}, K_{M_2}^{P_2}, K_{M_2}^{PP} \gg [Mg]_{free} \gg K_M^{PP}, K_M^{P_2}$	Mg_2E, $MgEMgP_i$, $MgE(MgP_i)_2$, Mg_2EMgPP_i (set 1)
2	$K_{M_4}, K_{M_2}^{P} \gg [Mg]_{free} \gg K_{M_3}, K_M^{P}, K_{M_2}^{P}, K_M^{P_2}, K_{M_2}^{P_2}, K_M^{PP}, K_{M_2}^{PP}$	Mg_3E, Mg_2EMgP_i, $Mg_2E(MgP_i)_2$, $Mg_2EMg_2PP_i$ (set 2)
3	$K_{M_4}, K_{M_2}^{P} \gg [Mg]_{free} \gg K_M^{PP}, K_M^{P_2}$	Mg_2E, $MgEMgP_i$, $MgE(MgP_i)_2$, Mg_2EMgPP_i
	$K_{M_3} \approx K_M^{P} \approx K_{M_2}^{P_2} \approx K_{M_2}^{PP} \equiv K_0$	Mg_3E, Mg_2EMgP_i, $Mg_2E(MgP_i)_2$, $Mg_2EMg_2PP_i$ (set 1 plus set 2)

Table VIII: Evaluation of Equilibrium and Rate Constants in Scheme II[a]

equilibrium constant	value	ref
K_1	2.0×10^{-7} M	b
K_3	4.8	b
K_5	4.5×10^{-3} M	b
K_7	5.2×10^{-4} M	b
k_1	3×10^7 M^{-1} s^{-1}	b
k_2	6 s^{-1}	b
k_3	1070 s^{-1}	b
k_4	222 s^{-1}	b
k_5	740 s^{-1}	b
k_6	1.64×10^5 M^{-1} s^{-1}	b
k_7	464 s^{-1}	b
k_8	8.9×10^5 M^{-1} s^{-1}	b
K_{PP}	1×10^4 M	c
K_B	5×10^{-2} M	c
K_A	2.7×10^{-4} M	d
K_{A_2}	6.3×10^{-3} M	d

[a] Conditions: 10 mM $[Mg]_{free}$, pH 7.0, 0.2 N KCl, and 25 °C. [b] This work. [c] Flodgaard & Fleron (1974). [d] Lambert & Watters (1957).

first following PP_i hydrolysis, P_c is given by $k_4/(k_4 + k_5)$, whereas if the electrophilic P_i is released second, then P_c is given by $k_4k_6[MgP_i]/[k_7(k_4 + k_5) + k_4k_6[MgP_i]]$, where $K_3 = k_3/k_4$, $K_5 = k_5/k_6$, and $K_7 = k_7/k_8$. We thus consider the lack of dependence of P_c on MgP_i concentration found by both Hackney (1980) and ourselves and the fact that $P_c < 1.0$ as strong evidence that the electrophilic P_i is released first. We have previously argued on the basis of mechanistic considerations that the low affinity P_i site was likely to contain the electrophile P_i (Hamm & Cooperman, 1978). That the electrophilic P_i is released first is at least consistent with this argument since it is reasonable to expect release to be more rapid from a low rather than a high-affinity site. Accordingly, in Scheme II, MgP_i is marked with an asterisk.

The conclusion that oxygen exchange occurs in the first released P_i allows us to derive the expression for $k_{cat,ex}$, the maximal steady-state rate constant for oxygen exchange (eq 11):

$$k_{cat,ex} = \left(\frac{k_5K_3}{K_3 + 1}\right)\left(\frac{4P_c}{4 - 3P_c}\right) \quad (11)$$

For Scheme II, the expressions for k_{cat} and K_m for PP_i hydrolysis are given by eq 12 and 13. These three equations

$$k_{cat,hyd} = \frac{k_3k_5k_7}{k_3k_5 + k_7(k_3 + k_4 + k_5)} \quad (12)$$

$$K_{m,hyd} = \frac{k_7[k_3k_5 + k_2(k_4 + k_5)]}{k_1[k_3k_5 + k_7(k_3 + k_4 + k_5)]} \quad (13)$$

(eq 11–13), when added to the five equations for K_1, K_3, K_5, K_7, and P_c, provide the eight equations necessary for calculation of all eight rate constants in Scheme II since all eight parameters have been determined experimentally. These rate constants are listed in Table VIII and lead to the following conclusions regarding the three reactions catalyzed by PPase: (1) For PP_i hydrolysis, steps 3, 5, and 7, corresponding to hydrolysis of PP_i on the enzyme surface and release of each of the product P_i's, respectively, are all partially rate determining. (2) For H_2O–P_i oxygen exchange, PP_i synthesis (step 4) is almost exclusively rate determining. (3) P_i–PP_i exchange has been found to be much slower than either of the other two reactions (Cohn, 1958; Janson et al., 1979), and here it is PP_i release from PPase (step 2) which is rate determining. It is worth noting that our own estimate for k_2 (6 s^{-1}) agrees quite well with a value of about 5 s^{-1}, which may be estimated from the measurements of Janson et al. (1979) and the saturation data in Figure 3.

In summary, the studies described in this paper have allowed us to define a unified scheme for PPase catalysis of PP_i hydrolysis, H_2O–P_i oxygen exchange, and PP_i–P_i equilibration in which three Mg^{2+} are required per active subunit and enabled us to evaluate the equilibrium and rate constants in this scheme.

References

Bagshaw, C. R., & Trentham, D. E. (1973) *Biochem. J. 133*, 323–328.

Bandurski, R. S., & Axelrod, B. (1951) *J. Biol. Chem. 193*, 405–410.

Butler, L. G., & Sperow, J. W. (1977) *Bioinorg. Chem. 7*, 141–150.

Cohn, M. (1958) *J. Biol. Chem. 230*, 369–379.

Cohn, M. (1979) in *NMR and Biochemistry* (Opella, S. J., & Lu, P., Eds.) pp 7–27, Marcel Dekker, New York.

Cohn, M., & Hu, A. (1978) *Proc. Natl. Acad. Sci. U.S.A. 75*, 200–203.

Cooperman, B. S., Chiu, N. Y., Bruckmann, R. H., Bunick, G. J., & McKenna, G. P. (1973) *Biochemistry 12*, 1665–1669.
Cooperman, B. S., Panackal, A., Springs, B., & Hamm, D. J. (1981) *Biochemistry 20*, 6051–6060.
Flodgaard, H., & Fleron, P. (1974) *J. Biol. Chem. 249*, 3465–3474.
Hackney, D. D. (1980) *J. Biol. Chem. 255*, 5320–5328.
Hackney, D. D., & Boyer, P. D. (1978) *Proc. Natl. Acad. Sci. U.S.A. 75*, 3133–3137.
Hackney, D. D., Stempel, K., & Boyer, P. D. (1980) *Methods Enzymol. 64*, 60–83.
Hamm, D. J., & Cooperman, B. S. (1978) *Biochemistry 17*, 4033–4040.
Heinrikson, R. L., Sterner, R., Noyes, C., Cooperman, B. S., & Bruckmann, R. H. (1973) *J. Biol. Chem. 248*, 2521–2528.
Janson, C. A., Degani, C., & Boyer, P. D. (1979) *J. Biol. Chem. 254*, 3743–3749.
Josse, J. (1966) *J. Biol. Chem. 241*, 1948–1955.
Knowles, J. R. (1980) *Annu. Rev. Biochem. 49*, 877–919.
Kunitz, M. (1952) *J. Gen. Physiol. 35*, 423–450.
Lambert, S. M., & Watters, J. I. (1957) *J. Am. Chem. Soc. 79*, 4262–4265, 5606–5608.
Moe, O. E., & Butler, L. G. (1972) *J. Biol. Chem. 247*, 7308–7314.
Randerath, K., & Randerath, E. (1967) *Methods Enzymol. 12*, 323–347.
Rapoport, T. A., Hohne, W. E., Reich, J. G., Heitmann, P., & Rapoport, S. M. (1972) *Eur. J. Biochem. 26*, 237–246.
Rapoport, T. A., Hohne, W. E., Heitmann, P., & Rapoport, S. M. (1973) *Eur. J. Biochem. 33*, 341–347.
Ridlington, J. W., & Butler, L. G. (1972) *J. Biol. Chem. 247*, 7303–7307.

Circular Dichroism Studies on the Interaction of Tryptophan Synthase with Pyridoxal 5′-Phosphate†

Hubert Balk, Inge Merkl, and Peter Bartholmes*

ABSTRACT: The interaction between the β_2 subunit of tryptophan synthase and the coenzyme pyridoxal 5′-phosphate (PLP) is characterized by induced circular dichroism (CD) in the near-UV (260–285 nm) and in the visible region (320–480 nm, extrinsic Cotton effect). Because of its high mean residue ellipticity ($[\theta]$ = 56 deg cm^2 dmol^{-1} for the isolated holo-β_2 subunit and 102 deg cm^2 dmol^{-1} for the α_2-holo-β_2 complex, respectively) the latter has been used to define different conformational states of the β_2 dimer via CD titrations. Fitting the obtained binding parameters to the known data from equilibrium dialysis leads to the result that the low-affinity state of the isolated β_2 subunit shows a 3 times greater rotational strength than the holoenzyme in the high-affinity state. The generation of the final CD amplitude is characterized by a rate constant intermediate between the values for the formation of the internal aldimine and for the regain of enzymatic activity. Interaction of the α_2-apo-β_2 bienzyme complex with the cofactor leads to a hyperbolic binding curve which is apparently free of contributions caused by unspecific PLP binding outside the active center. The determined dissociation constant of 9×10^{-7} M is in good agreement with the value of 1×10^{-6} M as obtained by equilibrium dialysis. Binding kinetics reveal a very slow process with a rate constant of 2.6×10^{-4} s^{-1}, significantly smaller than that for the regain of catalytic activity during reconstitution of the enzyme.

The isolated β_2 subunit of tryptophan synthase [L-serine hydro-lyase (adding indole)] (EC 4.2.1.20) from *Escherichia coli* catalyzes the last step of L-tryptophan biosynthesis in the presence of pyridoxal 5′-phosphate (PLP):[1]

L-serine + indole → L-tryptophan + H_2O

PLP and its analogues pyridoxine 5′-phosphate (PNP)[1] and *N*-(5′-phosphopyridoxyl)-L-serine (PPS)[1] bind cooperatively to the apo-β_2 subunit and noncooperatively to the α_2-apo-β_2 bienzyme complex (Bartholmes et al., 1976, 1980; Tschopp & Kirschner, 1980a).

When bound to proteins, a number of optically inactive low molecular weight compounds become optically active (Blauer, 1974). Such induced Cotton effects result from the interaction of the chromophore with the asymmetric environment provided by the binding site on the native protein. For instance, the enzyme-bound PLP chromophore of L-aspartate aminotransferase has been shown to be optically inactive as long as the corresponding polypeptide chain is unfolded in the presence of strong denaturants (Fasella & Hammes, 1964a,b). However, interaction of PLP with the active center in its native conformation leads to a strong extrinsic Cotton effect (Pötsch, 1976; Miles & Moriguchi, 1977) in the $\pi \rightarrow \pi^*$ transition of the aldimine chromophore. In this work, we report CD–equilibrium binding measurements and kinetic experiments with tryptophan synthase and PLP in order to shed some light on the alteration of structural parameters during cofactor binding and the successive generation of the catalytically active holoenzyme.

† From the Institut für Biophysik und Physikalische Biochemie, Universität Regensburg, D-8400 Regensburg, Federal Republic of Germany. *Received March 12, 1981; revised manuscript received June 11, 1981.* This work was supported by grants of the Deutsche Forschungsgemeinschaft and the Fonds der Chemischen Industrie. This work is dedicated to Dr. R. Jaenicke on the occasion of his 50th birthday.

[1] Abbreviations used: PLP, pyridoxal 5′-phosphate; CD, circular dichroism; ^{3}H, tritium; PNP, pyridoxine 5′-phosphate; PPS, *N*-(5′-phosphopyridoxyl)-L-serine.

0006-2960/81/0420-6391$01.25/0